

# Dynamical topological invariant for non-Hermitian Rice-Mele model

R. Wang,<sup>1</sup> X. Z. Zhang,<sup>2</sup> and Z. Song<sup>1,\*</sup>

<sup>1</sup>*School of Physics, Nankai University, Tianjin 300071, China*

<sup>2</sup>*College of Physics and Materials Science, Tianjin Normal University, Tianjin 300387, China*

We study a non-Hermitian Rice-Mele model without breaking time-reversal symmetry, with the non-Hermiticity arising from imbalanced hopping rates. The Berry connection, Berry curvature and Chern number are introduced in the context of biorthonormal inner product. It is shown that for a bulk system, although the Berry connection can be complex numbers, the Chern number is still quantized, as topological invariant. For an opened chain system, the mid-gap edge modes are obtained exactly, obeying the bulk-edge correspondence. Furthermore, we also introduce a local current in the context of biorthonormal inner product to measure the pumping charge generated by a cyclic adiabatic evolution. Analytical analysis and numerical simulation of the time evolution of the mid-gap states show that the pumping charge can be a dynamical topological invariant in correspondence with the Chern number. It indicates that the geometric concepts for Hermitian topological insulator can be extended to the non-Hermitian regime.

## I. INTRODUCTION

Nowadays, non-Hermitian Hamiltonian is no longer a forbidden regime in quantum mechanics since the discovery that a certain class of non-Hermitian Hamiltonians could exhibit the entirely real spectra [1, 2]. In non-Hermitian quantum mechanics, the reality of the spectrum, unitary evolution and probability conservation still hold if the Dirac inner product is replaced by biorthonormal inner product. The origin of the reality of the spectrum of a non-Hermitian Hamiltonian is the pseudo-Hermiticity of the Hamiltonian operator [3]. Such kinds of Hamiltonians possess a particular symmetry, i.e., it commutes with the combined operator  $\mathcal{PT}$ , but not necessarily with  $\mathcal{P}$  and  $\mathcal{T}$  separately. Here  $\mathcal{P}$  is a unitary operator, such as parity, translation, rotation operators etc., while  $\mathcal{T}$  is an anti-unitary operator, such as time-reversal operator. The combined symmetry is said to be unbroken if every eigenstate of the Hamiltonian is  $\mathcal{PT}$ -symmetric; then, the entire spectrum is real, while is said to be spontaneously broken if some eigenstates of the Hamiltonian are not the eigenstates of the combined symmetry. However, even within the unbroken symmetric region, many quantities, such as local particle probability, geometric phase of an adiabatic evolution of an eigenstate, etc., exhibit anomalous behavior in comparison with that in a Hermitian system. For instance, the biorthonormal expectation value of a local particle number operator and the geometric phase can be complex [4–6]. A natural question is that to what extent a non-Hermitian system could inherit the property of a Hermitian one by introducing biorthonormal inner product. In this paper, we investigate a non-Hermitian RM model, the Hermitian counterpart of which is a prototype system for topological matter.

We focus on the region without breaking time reversal symmetry, which supports fully real spectrum. We

investigate the topology of the degeneracy point by introducing the concepts of Berry connection, Berry curvature and Chern number in the context of biorthonormal inner product. In contrast to a Hermitian system, the Berry connection can be complex numbers. However, the Chern number is still quantized, as topological invariant to characterize the feature of energy band. For an opened chain system, the mid-gap edge modes are obtained exactly, that are identical to the ones in a Hermitian system. The bulk-edge correspondence still hold in the corresponding non-Hermitian SSH chain. Furthermore, we also introduce a local current in the context of biorthonormal inner product to measure the pumping charge generated by a cyclic adiabatic evolution, which is also defined by biorthonormal probability. Analytical analysis and numerical simulation of the time evolution of the mid-gap states show that the pumping charge can be a dynamical topological invariant in correspondence with the Chern number. Our results indicate that the geometric concepts for Hermitian topological insulator can be extended to the non-Hermitian regime.

This paper is organized as follows. In Section II, we present the model Hamiltonian and the solutions. In Section III, we introduce the concepts of Berry connection, Berry curvature, and Chern number for a non-Hermitian system. In Section IV, we calculate the Chern number in the concrete system. In Section V, we study the edge modes for the open chain system. Section VI devotes to the dynamical signature of topological feature of the degeneracy point. Finally, we give a summary and discussion in Section VII.

## II. MODEL HAMILTONIAN

We start our investigation by considering a non-Hermitian model with imbalanced hopping

$$H = \sum_{l=1}^{2N} [\kappa_{l,l+1} a_l^\dagger a_{l+1} + \kappa_{l+1,l} a_{l+1}^\dagger a_l - V (-1)^l a_l^\dagger a_l], \quad (1)$$

\* songtc@nankai.edu.cn

where  $\kappa_{l,l+1} = \frac{1+(-1)^l\delta}{2}\lambda(-1)^{l+1}$ ,  $\kappa_{l+1,l} = \frac{1+(-1)^l\delta}{2}\lambda(-1)^l$ . The spinless fermions satisfy the periodic boundary condition  $a_l \equiv a_{l+2N}$ . In this paper, we focus on the non-Hermitian system,  $\lambda \neq 1$  and  $> 0$ . It is a bipartite lattice, i.e., it has two sublattices  $A, B$  such that each site on lattice  $A$  has its nearest neighbors on sublattice  $B$ , and vice versa. The system is a variant of Hermitian SSH model by introducing the imbalanced hopping and staggered real potentials. The original Hermitian system at half-filling, proposed by Su, Schrieffer, and Heeger to model polyacetylene [7, 8], is the prototype of a topologically nontrivial band insulator with a symmetry protected topological phase [9, 10]. In recent years, it has been attracted much attention and extensive studies have been demonstrated [11–16].

The non-Hermiticity arises from asymmetry factor  $\lambda$ , which has been proposed to be realized in experiment [17]. We note that the Hamiltonian preserves time-reversal ( $\mathcal{T}$ ) symmetry. It has been shown that such type of system has entirely full real spectrum [18]. We introduce the Fourier transformations in two sub-lattices

$$a_l = \frac{1}{\sqrt{N}} \sum_k e^{ikj} \begin{cases} \beta_k, & l = 2j \\ \alpha_k, & l = 2j - 1 \end{cases}, \quad (2)$$

where  $j = 1, 2, \dots, N$ ,  $k = 2m\pi/N$ ,  $m = 0, 1, 2, \dots, N - 1$ . Spinless fermionic operators in  $k$  space  $\alpha_k, \beta_k$  are

$$\begin{cases} \beta_k = \frac{1}{\sqrt{N}} \sum_j e^{-ikj} a_l, & l = 2j \\ \alpha_k = \frac{1}{\sqrt{N}} \sum_j e^{-ikj} a_l, & l = 2j - 1 \end{cases}. \quad (3)$$

This transformation block diagonalizes the Hamiltonian due to its translational symmetry, i.e.,

$$H = \sum_{k \in [0, 2\pi)} H_k = \sum_{k \in [0, 2\pi)} \psi_k^\dagger h_k \psi_k, \quad (4)$$

satisfying  $[H_k, H_{k'}] = 0$ . Here  $H$  is rewritten in the Nambu representation with the basis

$$\psi_k = \begin{pmatrix} \alpha_k \\ \beta_k \end{pmatrix}, \quad (5)$$

and  $h_k$  is a  $2 \times 2$  matrix

$$h_k = \begin{pmatrix} V & \lambda\gamma_{-k} \\ \lambda^{-1}\gamma_k & -V \end{pmatrix}, \quad (6)$$

where  $\gamma_k = (\gamma_{-k})^\dagger = \frac{1}{2}[(1 - \delta) + (1 + \delta)e^{ik}]$ . The eigenvalues of  $h_k$  are  $|\varphi_\rho^k\rangle$  ( $\rho = \pm$ ) with eigenvalues

$$\varepsilon_\rho^k = \rho\sqrt{|\gamma_k|^2 + V^2}. \quad (7)$$

In the case of nonzero  $\lambda$ , we have all real eigenvalue. Let us denote the eigenvectors of a non-Hermitian Hamiltonian as

$$\begin{aligned} h_k |\varphi_\rho^k\rangle &= \varepsilon_\rho^k |\varphi_\rho^k\rangle, \\ h_k^\dagger |\eta_\rho^k\rangle &= \varepsilon_\rho^k |\eta_\rho^k\rangle, \end{aligned} \quad (8)$$

where the explicit expression of  $|\varphi_\rho^k\rangle$  and  $|\eta_\rho^k\rangle$  is

$$|\varphi_\rho^k\rangle = \frac{1}{\Omega_\rho} \begin{pmatrix} V + \varepsilon_\rho^k \\ \gamma_k \\ \lambda \end{pmatrix}, \quad (9)$$

$$|\eta_\rho^k\rangle = \frac{1}{\Omega_\rho} \begin{pmatrix} V + \varepsilon_\rho^k \\ \lambda\gamma_k \end{pmatrix}, \quad (10)$$

where the normalization factors  $\Omega_\rho = \sqrt{(V + \varepsilon_\rho^k)^2 + |\gamma_k|^2}$ . It is ready to check that biorthogonal bases  $\{|\varphi_\rho^k\rangle, |\eta_\rho^k\rangle\}$  ( $\rho = \pm$ ) obey the biorthogonal and completeness conditions

$$\langle \eta_{\rho'}^{k'} | \varphi_\rho^k \rangle = \delta_{kk'} \delta_{\rho\rho'}, \sum_{\rho, k} |\varphi_\rho^k\rangle \langle \varphi_\rho^k| = 1. \quad (11)$$

There are two Bloch bands from the eigenvalues of  $h_k$ , indexed by  $\rho = \pm$ . The band touching points occur at  $k_c$  when

$$\sqrt{|\gamma_{k_c}|^2 + V^2} = 0. \quad (12)$$

The solutions of above equation indicates the degeneracy point

$$\delta = 0, V = 0, \quad (13)$$

at  $k_c = \pi$ . The energy band structure is illustrated Fig. 1. We would like to stress that the origin is a degeneracy point rather than an exceptional point, although the system is a non-Hermitian system. The exceptional point appears only at the case with  $\lambda = 0$  and  $\infty$ , which is beyond our interest of this paper.

### III. GEOMETRIC QUANTITIES

The topological property of the degeneracy point for a Hermitian RM model is well established. It can be regarded as a monopole in the parameter space [11]. We will investigate what happens when the Hamiltonian is non-Hermitian. Before we focus on the concrete model, we first present a general formalism for a non-Hermitian system. In this section, we will develop a parallel theory for non-Hermitian case within the unbroken symmetry region. Without loss of generality, we neglect the detail of the model and consider a non-Hermitian spin-1/2 system in an external magnetic field, which can be described by the following Hamiltonian

$$h(k, q) = \mathbf{B}(k, q) \cdot \sigma, \quad (14)$$

where  $\mathbf{B}(k, q) = (B_x, B_y, B_z)$  is a complex magnetic field ( $B_x, B_y$  are complex, and  $B_z$  is real) and  $\sigma = (\sigma_x, \sigma_y, \sigma_z)$  is Pauli matrices

$$\sigma_x = \begin{pmatrix} 0 & 1 \\ 1 & 0 \end{pmatrix}, \sigma_y = \begin{pmatrix} 0 & -i \\ i & 0 \end{pmatrix}, \sigma_z = \begin{pmatrix} 1 & 0 \\ 0 & -1 \end{pmatrix}. \quad (15)$$

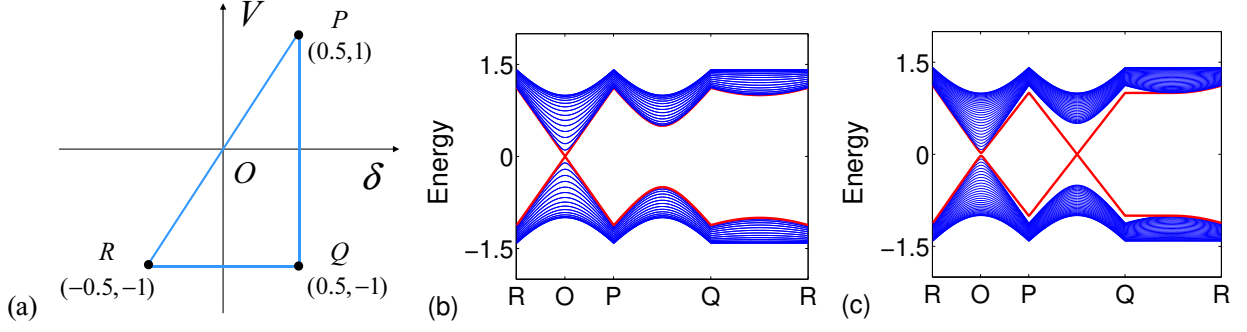


FIG. 1. (a) Schematics of  $V\delta$  plane. Energy spectrum for the system with parameters at the sides of triangle PQROP for (b) periodic boundary condition and (c) open boundary condition. The spectrum is independent of the imbalance factor  $\lambda$ . It indicates that two bands touch at point  $(0,0)$ . There are two mid-gap states for (a) with  $\delta > 0$ , which are shown to be edge states with identical wave functions for the standard SSH chain with  $\lambda = 1$  and  $V = 0$ .

The Hamiltonian is periodic with real  $q$  and  $k$ , i.e.,  $h(k, q) = h(k + k_0, q) = h(k, q + q_0)$ . Taking

$$\begin{cases} B_x = B \cos \phi \sin \theta \\ B_y = B \sin \phi \sin \theta \\ B_z = B \cos \theta \\ |\mathbf{B}| = B = \sqrt{(B_x)^2 + (B_y)^2 + (B_z)^2} \end{cases}, \quad (16)$$

with

$$\tan \phi = B_y/B_x, \cos \theta = B_z/B, \quad (17)$$

we rewrite the Hamiltonian as the form

$$h = B \begin{pmatrix} \cos \theta & \sin \theta e^{-i\phi} \\ \sin \theta e^{i\phi} & -\cos \theta \end{pmatrix}. \quad (18)$$

We note that  $\theta$  is real, while  $\phi$  is complex. In parallel, for the Hermitian conjugation counterpart

$$h^\dagger = B \begin{pmatrix} \cos \theta & \sin \theta e^{-i\phi^*} \\ \sin \theta e^{i\phi^*} & -\cos \theta \end{pmatrix}, \quad (19)$$

we have

$$\begin{aligned} h|\varphi_\rho\rangle &= \rho B|\varphi_\rho\rangle, \\ h^\dagger|\eta_\rho\rangle &= \rho B|\eta_\rho\rangle, \end{aligned} \quad (20)$$

where  $|\varphi_\rho\rangle$  and  $|\eta_\rho\rangle$  ( $\rho = \pm$ ) is the instantaneous eigenvectors of  $H$  and  $H^\dagger$ , respectively. Here the explicit expressions of these eigenvectors are

$$|\varphi_+\rangle = \begin{pmatrix} \cos \frac{\theta}{2} \\ \sin \frac{\theta}{2} e^{i\phi} \end{pmatrix}, |\varphi_-\rangle = \begin{pmatrix} -\sin \frac{\theta}{2} \\ \cos \frac{\theta}{2} e^{i\phi} \end{pmatrix}, \quad (21)$$

and

$$|\eta_+\rangle = \begin{pmatrix} \cos \frac{\theta}{2} \\ \sin \frac{\theta}{2} e^{i\phi^*} \end{pmatrix}, |\eta_-\rangle = \begin{pmatrix} -\sin \frac{\theta}{2} \\ \cos \frac{\theta}{2} e^{i\phi^*} \end{pmatrix}, \quad (22)$$

which obey the biorthonormal relations

$$\langle \eta_\rho | \varphi_{\rho'} \rangle = \langle \varphi_{\rho'} | \eta_\rho \rangle = \delta_{\rho\rho'}. \quad (23)$$

We define the Berry connection  $A_\sigma^\rho$  ( $\sigma = k, q$ ) and the Berry curvature  $\Omega_{kq}^\rho$  in the context of biorthonormal inner product

$$A_\sigma^\rho = -i \langle \eta_\rho | \nabla_\sigma | \varphi_\rho \rangle, \Omega_{kq}^\rho = \partial_k A_q^\rho - \partial_q A_k^\rho, \quad (24)$$

Similar to the Hermitian case,  $A_\sigma^\rho$  is gauge dependent while  $\Omega_{kq}^\rho$  is not. Accordingly Chern number can be defined as

$$c_\rho = \frac{1}{2\pi} \int_k^{k+k_0} \int_q^{q+q_0} \Omega_{kq}^\rho dk dq. \quad (25)$$

For well defined  $A_k^\rho$  and  $A_q^\rho$ , the Chern number can be rewritten as the form

$$c_\rho = \frac{1}{2\pi} \oint_{\partial D} \mathbf{A}^\rho \cdot d\mathbf{r}, \quad (26)$$

where  $\mathbf{A}^\rho = A_k^\rho \hat{k} + A_q^\rho \hat{q}$ ,  $r = k\hat{k} + q\hat{q}$ . Here  $\hat{q}$  and  $\hat{k}$  are unit vectors, and  $\partial D$  (boundary of the domain  $D$ , which covers the square of  $k_0 \times q_0$ ) is the path of the integral. We concern whether  $c_\rho$  is still quantized for real  $|\mathbf{B}|$  in the non-Hermitian system as a topological invariant. We will investigate these issues based on a concrete model.

#### IV. CHERN NUMBER

In this section, we will calculate the explicit expressions of the geometric quantities for the non-Hermitian RM model. The Bloch Hamiltonian is periodic through the periodic functions  $V(q) = V(q + 2\pi)$  and  $\delta(q) = \delta(q + 2\pi)$ . When  $q$  sweeps over a period, the system experiences a loop in the  $V\delta$  plane. For this concrete model, we have the explicit form of magnetic field

$$\begin{cases} B_x = \frac{1}{2} (\lambda \gamma_{-k} + \lambda^{-1} \gamma_k), \\ B_y = \frac{i}{2} (\lambda \gamma_{-k} - \lambda^{-1} \gamma_k), \\ B_z = V, \end{cases} \quad (27)$$

and

$$B = \sqrt{|\gamma_k|^2 + V^2}. \quad (28)$$

Obviously, field  $\mathbf{B}$  is periodic vector,  $\mathbf{B}(q, k) = \mathbf{B}(q + 2\pi, k) = \mathbf{B}(q, k + 2\pi)$ . In the following we only focus on the lower band, neglecting the band index for the geometric quantity. Direct derivations show that

$$\mathbf{A} = -i\langle\eta^k|\partial_q|\varphi^k\rangle\hat{q} - i\langle\eta^k|\partial_k|\varphi^k\rangle\hat{k} \quad (29)$$

with

$$\langle\eta|\partial_\sigma|\varphi\rangle = \frac{1}{2}\left[\frac{1}{2}\sin\theta(\partial_\sigma\theta)(1 - e^{2i\text{Re}\phi}) + i(1 + \cos\theta)(\partial_\sigma\phi)e^{2i\text{Re}\phi}\right], \quad (30)$$

where  $\hat{q}$  and  $\hat{k}$  are unit vectors for parameters  $\sigma = q, k$  respectively, and the angles are

$$\phi = \arctan\left[\frac{i(\lambda\gamma_{-k} - \lambda^{-1}\gamma_k)}{(\lambda\gamma_{-k} + \lambda^{-1}\gamma_k)}\right], \quad (31)$$

$$\theta = \arccos\left(\frac{V}{\sqrt{|\gamma_k|^2 + V^2}}\right). \quad (32)$$

We note that  $\theta$  is real, while  $\phi$  is complex. In contrast to a Hermitian case, Berry connection  $\mathbf{A}$  is complex as expected, which accords with the violation of the conservation of Dirac probability. Apparently, the Berry curvature can be directly obtained by the definition in Eq. (24), and then the Chern number. However, it is impossible to get all the Berry curvatures for a given loop through a single expression of  $\mathbf{A}$ , since the wave functions  $|\varphi\rangle$  and  $|\eta\rangle$  are not smooth and single valued everywhere.

For instance, when taking  $\theta = 0$ , (or  $B_y = B_x = 0$ , and  $B_z > 0$ ) we have

$$|\varphi\rangle = \begin{pmatrix} 0 \\ e^{i\phi} \end{pmatrix}, |\eta\rangle = \begin{pmatrix} 0 \\ e^{i\phi^*} \end{pmatrix}. \quad (33)$$

where  $\varphi$  is not well-defined, or indefinite. So  $|\varphi\rangle$  and  $|\eta\rangle$  have singularity at  $\mathbf{B} = (0, 0, B_z)$  with  $B_z > 0$ . We can choose another gauge by multiplying  $|\varphi\rangle$  and  $|\eta\rangle$  by  $e^{-i\text{Re}\phi}$ . Then the wave function is smooth and single valued everywhere except at the south pole, i.e.,  $\varphi$  is not well-defined, or indefinite at  $\theta = \pi$ . For a given loop, one should choose one or two specific gauges, or expressions of  $|\varphi\rangle$  and  $|\eta\rangle$  in order to calculate the Chern number. If a set of proper chosen wave functions  $\{|\varphi\rangle, |\eta\rangle\}$  are well-defined for a given loop, the Chern number is zero. If a loop requires two different gauges, the Chern number is nonzero. Obviously, the difference between the Berry connections  $\mathbf{A}$  in two gauges is  $\nabla_{\mathbf{R}}\text{Re}\phi$ , and thus Chern number are definitely real.

We choose four typical loops, involving: (a) quadrants I and II ( $V > 0$ ); (b) quadrants III and IV ( $V < 0$ ); (c) one of four quadrants, or quadrants I and IV ( $\delta > 0$ ), or quadrants II and III ( $\delta < 0$ ), and (d) quadrants I, II, III, and IV (enclosing the origin). For the cases (a-c), one can take the gauge as

$$\begin{aligned} & \text{(a)} : |\varphi\rangle, |\eta\rangle; \\ & \text{(b)} : e^{i\text{Re}\phi}|\varphi\rangle, e^{i\text{Re}\phi}|\eta\rangle; \\ & \text{(c)} : |\varphi\rangle, |\eta\rangle; \\ & \quad \text{or } e^{i\text{Re}\phi}|\varphi\rangle, e^{i\text{Re}\phi}|\eta\rangle, \end{aligned} \quad (34)$$

while one need two gauges for (d) as

$$\begin{aligned} & \text{(dI)} : |\varphi\rangle, |\eta\rangle, \quad (V > 0); \\ & \text{(dII)} : e^{i\text{Re}\phi}|\varphi\rangle, e^{i\text{Re}\phi}|\eta\rangle, \quad (V < 0). \end{aligned} \quad (35)$$

We conclude from this analysis that the Chern number is nonzero when the loop encloses the origin. Explicitly, with the Eq. (26), we have

$$\begin{aligned} c &= \frac{1}{2\pi} \left( \oint_{\partial D_I} \mathbf{A}_I + \oint_{\partial D_{II}} \mathbf{A}_{II} \right) \cdot d\mathbf{r} \\ &= \frac{1}{2\pi} \oint_{\partial D_I} (\mathbf{A}_I - \mathbf{A}_{II}) \cdot d\mathbf{r} \\ &\neq 0, \end{aligned} \quad (36)$$

where the subindex of  $\mathcal{A}_I$  and  $\mathcal{A}_{II}$  distinguish  $(|\varphi\rangle, |\eta\rangle)$  from  $(e^{i\text{Re}\phi}|\varphi\rangle, e^{i\text{Re}\phi}|\eta\rangle)$  respectively, when we define the Berry connection.

To demonstrate the result, we consider a loop in the form

$$\begin{cases} \delta = \delta_c + r \cos q \\ V = V_c + r \sin q \end{cases} \quad (37)$$

which is a circle in  $V\delta$  plane with radius  $r$ , centered at  $(\delta_c, V_c)$ . The Chern number can be obtained as

$$c = \begin{cases} 0, & \delta_c^2 + V_c^2 > r^2 \\ 1, & \delta_c^2 + V_c^2 < r^2 \end{cases}, \quad (38)$$

i.e., Chern number is zero if the loop does not encircle the degeneracy point, while is nonzero if encircle the degeneracy point. In addition, if we take  $q \rightarrow -q$ , we will get  $c \rightarrow -c$ , which means that one gets opposite Chern number for the same loop but with opposite direction. We schematically illustrate this loop in Fig. 3(a).

It shows that the degeneracy point still has topological feature in a non-Hermitian system even though the Berry connection may be complex. The underlying mechanism of the quantization of the Chern number for a non-Hermitian system is that the single-valuedness of the wave function is always true no matter the system is Hermitian or not.

## V. EDGE-MODE OPERATORS

In a Hermitian SSH model, the degenerate zero modes take the role of topological invariant for opened chain. In this section, we investigate the similar feature for non-Hermitian RM model. Considering the RM model with an open boundary condition, the Hamiltonians read

$$\begin{aligned} H_{\text{CH}} &= H - M, \\ M &= \kappa_{2N,1}a_{2N}^\dagger a_1 + \kappa_{1,2N}a_1^\dagger a_{2N}, \end{aligned} \quad (39)$$

which represents the original system with broken the coupling across two sites  $(2N, 1)$ . We introduce a pair of

edge-mode operators  $\bar{A}_{L,R}$  in the infinite  $N$  limit, which are defined as

$$\bar{A}_L = \frac{1}{\sqrt{\Omega}} \sum_{j=1}^N \left( \frac{\delta-1}{\delta+1} \right)^{N-j} a_{2j}^\dagger, \quad (40)$$

$$\bar{A}_R = \frac{1}{\sqrt{\Omega}} \sum_{j=1}^N \left( \frac{\delta-1}{\delta+1} \right)^{j-1} a_{2j-1}^\dagger, \quad (41)$$

where  $\Omega = \{1 - [(\delta-1)/(\delta+1)]^{2N}\} / \{1 - [(\delta-1)/(\delta+1)]^2\}$ . It is easy to check that

$$[\bar{A}_L, H_{CH}] = V\bar{A}_L, \quad (42)$$

$$[\bar{A}_R, H_{CH}] = -V\bar{A}_R, \quad (43)$$

which ensures that

$$H_{CH}\bar{A}_L|\text{Vac}\rangle = -V\bar{A}_L|\text{Vac}\rangle, \quad (44)$$

$$H_{CH}\bar{A}_R|\text{Vac}\rangle = V\bar{A}_R|\text{Vac}\rangle, \quad (45)$$

$$H_{CH}\bar{A}_L\bar{A}_R|\text{Vac}\rangle = 0 \times \bar{A}_L\bar{A}_R|\text{Vac}\rangle. \quad (46)$$

Here  $|\text{Vac}\rangle$  is the vacuum state of fermion operator, i.e.,  $a_l|\text{Vac}\rangle = 0$ . Obviously, states  $\bar{A}_{L,R}|\text{Vac}\rangle$  and  $\bar{A}_L\bar{A}_R|\text{Vac}\rangle$  are the eigenstates of  $H_{CH}$  with eigen energies  $\mp V$  and 0, respectively.

In parallel, we can also define the biorthogonal conjugation operators

$$A_L = \frac{1}{\sqrt{\Omega}} \sum_{j=1}^N \left( \frac{\delta-1}{\delta+1} \right)^{N-j} a_{2j}, \quad (47)$$

$$A_R = \frac{1}{\sqrt{\Omega}} \sum_{j=1}^N \left( \frac{\delta-1}{\delta+1} \right)^{j-1} a_{2j-1}, \quad (48)$$

which satisfy the canonical commutation relations

$$\{A_\mu, \bar{A}_\nu\} = \delta_{\mu\nu}, \{A_\mu, A_\nu\} = \{\bar{A}_\mu, \bar{A}_\nu\} = 0, \quad (49)$$

with the indices  $\mu, \nu = L, R$ . Similarly, we have

$$[A_L^\dagger, H_{CH}^\dagger] = V A_L^\dagger, [A_R^\dagger, H_{CH}^\dagger] = -V A_R^\dagger, \quad (50)$$

which indicate that states  $A_{L,R}^\dagger|\text{Vac}\rangle$  and  $A_L^\dagger A_R^\dagger|\text{Vac}\rangle$  are the eigenstates of  $H_{CH}^\dagger$  with eigen energies  $\mp V$  and 0, respectively.

A surprising fact is that  $A_\mu^\dagger = \bar{A}_\mu$ , which does not hold true in general since  $H_{CH} \neq H_{CH}^\dagger$ . It is due to the special eigenstates of a particular model. This feature allows us to treat the edge modes in the framework of Hermitian regime. The biorthonormal and Dirac probabilities of the edge modes are the same and can be expressed as

$$\mathcal{P}_\mu(l) = \langle \text{Vac} | A_\mu a_l^\dagger a_l A_\mu^\dagger | \text{Vac} \rangle. \quad (51)$$

or explicit form

$$\mathcal{P}_L(l) = \begin{cases} \frac{1}{\Omega} \left( \frac{\delta-1}{\delta+1} \right)^{2N-l}, & l = 2j \\ 0, & l = 2j-1 \end{cases}, \quad (52)$$

and

$$\mathcal{P}_R(l) = \begin{cases} 0, & l = 2j \\ \frac{1}{\Omega} \left( \frac{\delta-1}{\delta+1} \right)^{l-1}, & l = 2j-1 \end{cases}, \quad (53)$$

which obey the normalization condition  $\sum_l \mathcal{P}_\mu(l) = 1$ . We note that the edge modes are independent of  $\lambda$  and  $V$ , identical to that for the standard SSH chain ( $V = 0$  and  $\lambda = 1$ ). In contrast to the standard SSH chain, the eigenvalues of edged modes can be nonzero. The profiles of the edge modes are illustrated schematically in Fig. 2.

Based on the above analysis, it turns out that the bulk system exhibits the similar topological feature when taking  $V = 0$ . In Hermitian systems, the existence of edge modes is intimately related to the bulk topological quantum numbers, which is referred as the bulk-edge correspondence relations [19–22]. We are interested in the generalization of the bulk-edge correspondence to this non-Hermitian system. Previous works show that when sufficiently weak non-Hermiticity is introduced to topological insulator models, the edge modes can retain some of their original characteristics [23, 24]. Similarly, we can get the same conclusion for the case with  $V = 0$ , if we define the Zak phase in the framework of biorthonormal inner product, demonstrating the bulk-edge correspondence.

## VI. PUMPING CHARGE

In a Hermitian system, the physical meaning of Chern number is well known. In a Hermitian RM model, it has been shown that the adiabatic particle transport over a time period takes the form of the Chern number and it is quantized [11]. The pumped charge counts the net number of degenerate point enclosed by the loop. For example, consider a time-dependent Hamiltonian, which varies adiabatically along the circle in Eq. (37). After a period of time, the particle transport for the half-filled ground state equals to the Chern number of the loop in Eq. (38). In the above, we have shown that a non-Hermitian system can exhibit the similar topological feature as that in a Hermitian system. The Chern number as the topological invariant defined in the context of biorthonormal inner product. In parallel, such a Chern number should have the similar physical meaning.

Actually, one can rewrite Eq. (26) in the form

$$\begin{aligned} c &= \oint \left( \frac{\partial \mathcal{Z}}{\partial \delta} d\delta + \frac{\partial \mathcal{Z}}{\partial V} dV \right) \\ &= \int_0^T \left( \frac{\partial \mathcal{Z}}{\partial \delta} \dot{\delta} + \frac{\partial \mathcal{Z}}{\partial V} \dot{V} \right) dt, \end{aligned} \quad (54)$$

where  $\mathcal{Z}$  is Zak phase

$$\mathcal{Z} = \frac{i}{2\pi} \int_0^{2\pi} \langle \eta^k | \partial_k | \varphi^k \rangle dk, \quad (55)$$

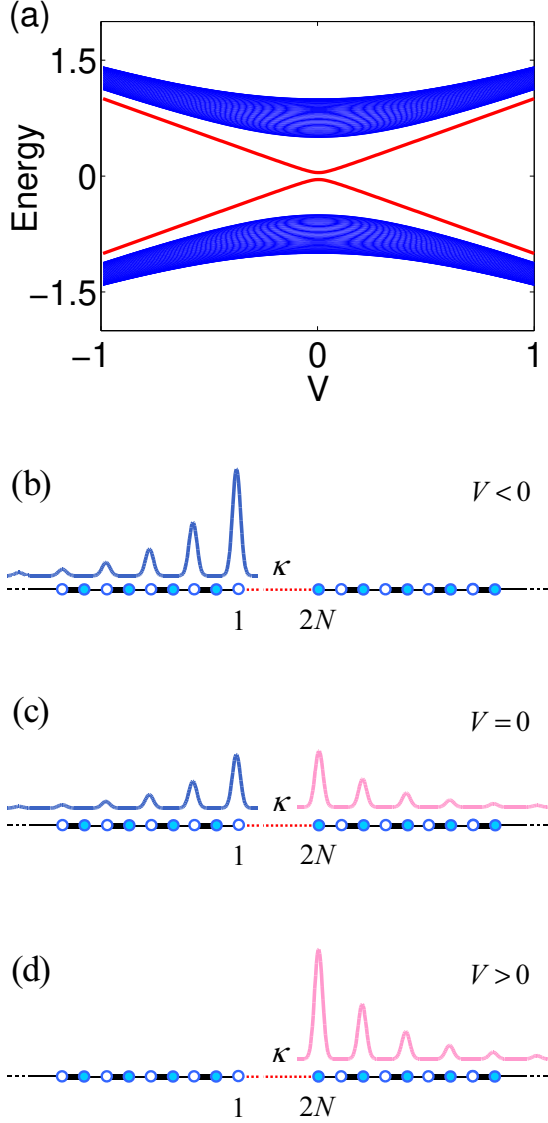


FIG. 2. (a) Plot of the spectrum of  $H_\kappa$  in Eq. (58) with  $N = 50$ ,  $\delta = 0.5$ ,  $\kappa = 0.05$ , and  $\lambda = 1.5$ . Comparing to that in Fig. 1(c), the level crossing becomes avoided level crossing around  $V = 0$ , at which two types of edge modes are hybridized. (b) and (d) are schematics for two edge modes. (c) The superpositions of the two become mid-gap states when  $V$  turns to zero. When varying  $V$  from  $-1$  to  $1$  adiabatically, (b) will evolve to (c), then (d), resulting an adiabatic particle transport from the leftmost of the chain to the rightmost.

defined in the context of biorthonormal inner product. Here  $V$  and  $\delta$  is periodic function of time  $t$  and the sub-index is neglected for simplicity. Furthermore, we can find out the physical meaning of the Chern number by the relation

$$c = \int_0^T \mathcal{J}(t) dt, \quad (56)$$

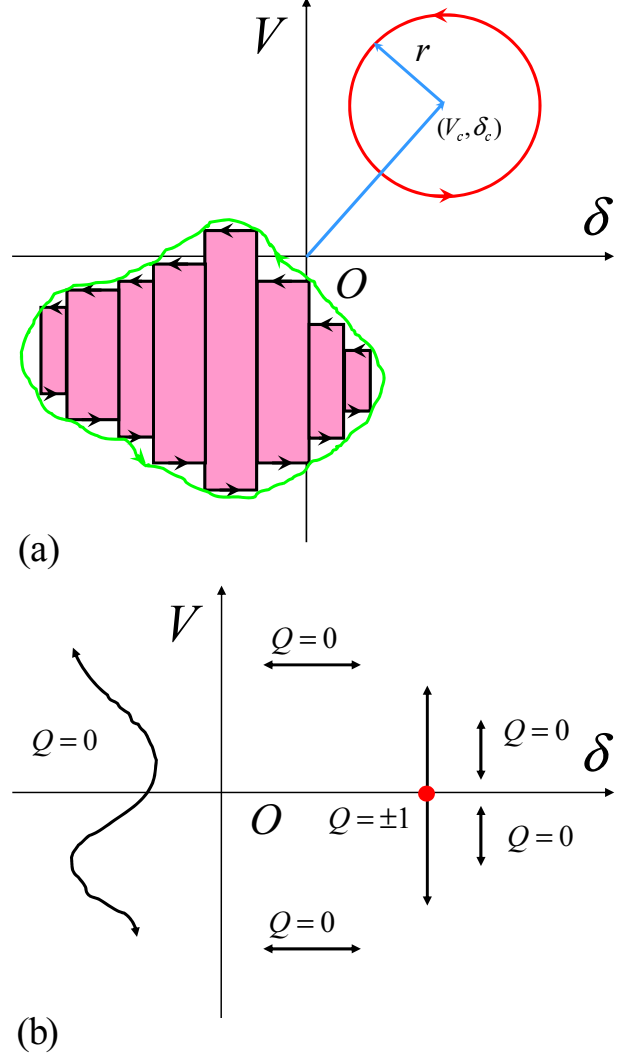


FIG. 3. (a) Schematics of a simple loop represented in Eq. (38). For an arbitrary loop, it can be decomposed into many rectangular loops. The Chern number of an arbitrary loop is the sum of all the Chern numbers of the rectangles. (b) Six types of segments which can be used to construct any kinds of loops. It turns out that only the vertical one passing through the red dot has nonzero charge transport across the two ends of the chain (see text and Fig. 2(b)-(d)).

where

$$\mathcal{J} = \frac{i}{2\pi} \int_0^{2\pi} [(\partial_t \langle \eta^k |) \partial_k | \varphi^k \rangle - (\partial_k \langle \eta^k |) \partial_t | \varphi^k \rangle] dk \quad (57)$$

is the adiabatic current of biorthonormal version. Then  $c$  is pumped charge of all channel  $k$  driven by the time-dependent Hamiltonian varying in a period.

This conclusion is obtained for a model Hamiltonian with translational symmetry. Next, we consider this issue based on the edge states for the chain system. Based on the exact expression of the edge states, we have known

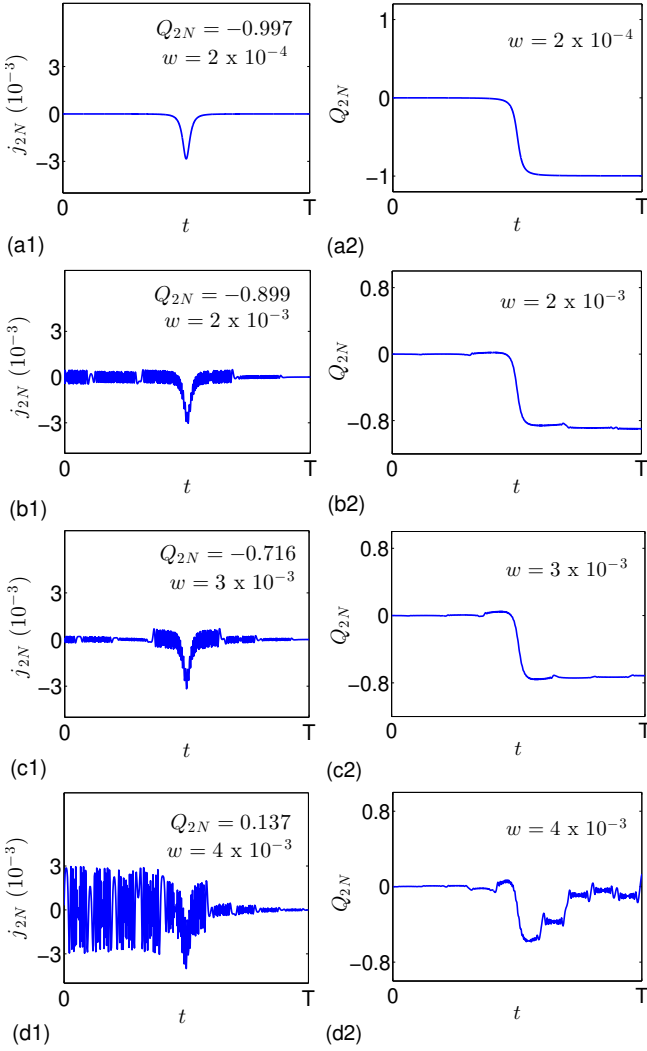


FIG. 4. Numerical simulations of particle transport across two ends of the chain current obtained by exact diagonalization, driven by the time-dependent parameter  $V = 1 - 2\omega t$ ,  $t \in [0, T = \omega^{-1}]$ . Plots of the current (a1-d1) and charge accumulation as function of time (a2-d2) for several typical speed  $\omega$ , indicated in the figures. The total charge transfer during the interval  $[0, \omega^{-1}]$  is also indicated in each figure. We note that the result accords with our prediction well when the speed is slow enough in (a1, b1). As  $\omega$  increases, the deviation becomes larger and larger. In the case of (a4, b4), the accumulated charge becomes positive, which is qualitatively different from the adiabatic process. The parameters of the system are  $N = 10$ ,  $\delta = 0.5$ ,  $\kappa = 0.05$ , and  $\lambda = 1.5$ .

that only  $\delta$  can change the distribution of the probability. Specifically, for a given  $V > 0$ , if we vary  $\delta$  from  $\delta_0 > 0$  to  $-\delta_0$  adiabatically, the state  $\bar{A}_L |\text{Vac}\rangle$  will evolve to  $\bar{A}_R |\text{Vac}\rangle$ . Then particle will transport adiabatically from the rightmost of the chain to the leftmost. Remarkably, one can get the same result from an alternative way. We consider a system with additional weak tunneling  $\kappa$  between two ends. The corresponding Hamiltonian has the

form

$$H_\kappa = H_{\text{CH}} + \kappa M, \quad (58)$$

which is schematically illustrated in Fig. 2 and the structure of spectrum of  $H_\kappa$  is plotted in Fig. 2(a). We note that the weak tunneling  $\kappa$  hybridize two edge  $\bar{A}_L |\text{Vac}\rangle$  and to  $\bar{A}_R |\text{Vac}\rangle$  states when  $\delta > 0$  and  $V$  around 0. For a given  $\delta > 0$ , if we vary  $V$  from  $V_0 > 0$  to  $-V_0$  adiabatically, the state  $\bar{A}_L |\text{Vac}\rangle$  will evolve to  $\bar{A}_R |\text{Vac}\rangle$ . Then a particle will transport adiabatically from the rightmost of the chain to the leftmost. Fig. 2(b) and (d), illustrate this point. During this process, particle should pass through the connection of two ends rather than the bulk region of the chain. This transport can be detected by watching the current across two ends. The accumulated charge of the current should be integer.

Inspired by these results we expect that the hidden topology behind the non-Hermitian model can be unveiled by the pumping charge with the respect to the mid-gap edge mode rather than all the energy levels. As illustrated in Fig. 3(a), the pumping charge is the sum of all the pumping charges obtained by an infinite rectangular loops. The pumping charge of a rectangular loop is simply determined by the positions of two vertical sides. Therefore, we can conclude that the pumping charge of an edge state for an arbitrary loop equals to the corresponding Chern number of the loop.

To characterize the charge transfer quantitatively, we developed the concept of the biorthonormal current in a non-Hermitian tight-binding model. In the following, only single-particle case is concerned. We begin with the rate of change of the biorthonormal probability  $\rho_l$  at an arbitrary site  $l$  for given eigenstate  $(|\varphi(t)\rangle, |\eta(t)\rangle)$  at instant  $t$ , which can be expressed as

$$\begin{aligned} \frac{d\rho_l}{dt} &= \frac{d\langle\eta(t)|l\rangle\langle l|\varphi(t)\rangle}{dt} \\ &= \frac{1}{i}\langle\eta(t)|[|l\rangle\langle l|, H]|\varphi(t)\rangle \end{aligned} \quad (59)$$

where  $|l\rangle = a_l^\dagger |\text{Vac}\rangle$ . For the concerned Hamiltonian we have

$$\frac{d\rho_l}{dt} = j_l - j_{l-1}, \quad (60)$$

where

$$j_l = \frac{1}{i}\langle\eta(t)|(\kappa_{l,l+1}|l\rangle\langle l+1| - \kappa_{l+1,l}|l+1\rangle\langle l|)|\varphi(t)\rangle. \quad (61)$$

The quantity  $j_l$  refers to the biorthonormal current across sites  $l$  and  $l+1$ . The accumulated charge passing the site  $l$  during the period  $T$  is

$$Q_l = \int_0^T (j_l - j_{l-1}) dt. \quad (62)$$

We consider the case by taking  $V = V_0(1 - 2\omega t)$  with  $\omega \ll 1$ , and

$$|\varphi(0)\rangle = \bar{A}_L |\text{Vac}\rangle, \quad |\eta(0)\rangle = A_L^\dagger |\text{Vac}\rangle. \quad (63)$$

According to the analysis above, if  $t$  varies from 0 to  $T = \omega^{-1}$ ,  $Q_I$  should be 1 or  $-1$ , which is consistent with the direction of the loop. To examine how the scheme works in practice, we simulate the quasi-adiabatic process by computing the time evolution numerically for finite system. In principle, for a given initial eigenstate  $|\psi(0)\rangle$ , the time evolved state under a Hamiltonian  $H_\kappa(t)$  is

$$|\Phi(t)\rangle = \mathcal{T}\{\exp(-i \int_0^t H_\kappa(t) dt) |\psi(0)\rangle\}, \quad (64)$$

where  $\mathcal{T}$  is the time-ordered operator. In low speed limit  $\omega \rightarrow 0$ , we have

$$f(t) = |\langle \bar{\psi}(t) | \Phi(t) \rangle| \rightarrow 1, \quad (65)$$

where  $\langle \bar{\psi}(t) |$  is the corresponding instantaneous eigenstate of  $H_\kappa^\dagger(t)$ . The computation is performed by using a uniform mesh in the time discretization for the time-dependent Hamiltonian  $H_{CH}(t)$ . In order to demonstrate a quasi-adiabatic process, we keep  $f(t) > 0.9985$  during the whole process by taking sufficient small  $\omega$  (see the case (a1, b1) in Fig. 4). Fig. 4 plots the simulations of particle current and the corresponding total probability for several typical cases, in order to see to what extent the process can be regarded as a quasi-adiabatic one. It shows that the obtained dynamical quantities are in close agreement with the expected Chern number.

## VII. SUMMARY

In summary, we have analyzed a one-dimensional non-Hermitian RM model that exhibits the similar topological features of a Hermitian one within the time-reversal symmetry-unbroken regions, in which the Berry connection, Berry curvature, Chern number, current, and pumped charge, etc., are defined in the context of biorthonormal inner product. We also examined the dynamical signature for topological invariant, which is pumped charge driven by the parameters. The underlying mechanism of our finding is that if a non-Hermitian system is pseudo-Hermitian and the Hermitian counterpart of its is topological within the unbroken symmetric region, such a non-Hermitian system inherits the same topological characterization of the counterpart.

## ACKNOWLEDGMENTS

We acknowledge the support of the CNSF (Grant No. 11374163).

- 
- [1] C. M. Bender and S. Boettcher, Phys. Rev. Lett. **80**, 5243 (1998).
  - [2] C. M. Bender, D. C. Brody and H. F. Jones, Phys. Rev. Lett. **89**, 270401 (2002).
  - [3] A. Mostafazadeh, J. Math. Phys. **43**, 205 (2002).
  - [4] C. M. Bender, Making sense of non-Hermitian Hamiltonians. Rep. Prog. Phys. **70**, 947–1018 (2007).
  - [5] F. G. Scholtz, H. B. Geyer and F. J. W. Hahne, Quasi-Hermitian operators in quantum mechanics and the variational principle, Ann. Phys. (NY) **213**, 74–101 (1992).
  - [6] D. P. Musumbu, H. B. Geyer and W. D. Heiss, J. Phys. **40**, 75 (2007).
  - [7] W. P. Su, J. R. Schrieffer, and A. J. Heeger, Phys. Rev. Lett. **42**, 1698 (1979).
  - [8] J. R. Schrieffer, *The Lesson of Quantum Theory* (North Holland, Amsterdam, 1986).
  - [9] Shinsei Ryu and Yasuhiro Hatsugai, Phys. Rev. Lett. **89**, 077002 (2002).
  - [10] Xiao-Gang Wen, Phys. Rev. B **85**, 085103 (2012).
  - [11] D. Xiao, M. C. Chang, and Q. Niu, Rev. Mod. Phys. **82**, 1959 (2010).
  - [12] M. Z. Hasan and C. L. Kane, Rev. Mod. Phys. **82**, 3045 (2010); X. -L. Qi and S. -C. Zhang, ibid. **83**, 1057 (2011).
  - [13] P. Delplace, D. Ullmo, and G. Montambaux Phys. Rev. B **84**, 195452 (2011).
  - [14] Linhu Li, Zhihao Xu, and Shu Chen, Phys. Rev. B **89**, 085111 (2014).
  - [15] Linhu Li and Shu Chen, Phys. Rev. B **92**, 085118 (2015).
  - [16] S. Lin, and Z. Song, Phys. Rev. A **96**, 052121 (2017).
  - [17] S. Longhi, Phys. Rev. A **95**, 062122 (2017).
  - [18] X. Z. Zhang and Z. Song, Ann. Physics **339**, 109–121 (2013).
  - [19] D. J. Thouless, *Topological Quantum Numbers in Non-relativistic Physics* (World Scientific, Singapore, 1998).
  - [20] M. Z. Hasan and C. L. Kane, Rev. Mod. Phys. **82**, 3045 (2010).
  - [21] X.-L. Qi and S.-C. Zhang, Rev. Mod. Phys. **83**, 1057 (2011).
  - [22] L. Lu, J. D. Joannopoulos, and M. Soljačić, Nat. Photonics **8**, 821 (2014).
  - [23] K. Esaki, M. Sato, K. Hasebe, and M. Kohmoto, Phys. Rev. B **84**, 205128 (2011).
  - [24] Y. C. Hu and T. L. Hughes, Phys. Rev. B **84**, 153101 (2011).